Solid State Phenomena
ISSN: 1662-9779, Vol. 388, pp 57-66
doi:10.4028/p-9RDkIt

Submitted: 2025-12-22
Revised: 2026-02-15
Accepted: 2026-02-19
Online: 2026-04-15

Theoretical and Experimental Forming Limit Evaluation of High-Strength Steels up to 1500 MPa

Borbely Richard[1,2,a*],Keresztes Robert Zsolt[2,b] and Beres Gabor Jozsef[1,c]

[1]Innovative Vehicles and Materials Department, John von Neumann University, Hungary

[2]Doctoral School of Technical Sciences, Hungarian University of Agriculture and Life Sciences, Hungary

[a*]borbely.richard@nje.hu, [b]keresztes.robert.zsolt@uni-mate.hu, [c]beres.gabor@nje.hu

Keywords: high-strenght steels, forming limit curve, formability.

Abstract. The prediction of sheet failure remains a highly relevant topic in metal forming research, particularly in relation to the experimental and theoretical determination of forming limit curves (FLCs). While the experimental construction of FLCs is a well-established but time-consuming process, theoretical and numerical approaches provide a more efficient alternative. However, their accuracy must be critically assessed, all the time. In this work, the formability of steel sheet with tensile strengths of 1500 MPa is investigated by combining experimental Nakajima tests with theoretical predictions of FLCs. Previous studies, such as models by Abspoel, Swift, Hill etc. have not addressed such high strength levels, where the diffuse and local neck points are quite close, leaving open the question of whether existing approaches remain valid for these materials. To provide a reference baseline, additional tests and calculations were also performed on lower-strength steel sheet (DP800). Our results show that the FLC points can be well estimated by two different theories in the positive quadrant, but there are noticeable differences between the measured and calculated values close to the plane strain point.

Introduction

The prediction of sheet failure has long been a central topic in metal forming research. The ability to accurately determine the forming limits of sheet materials is essential for the optimization of forming processes and for preventing failure during production. Early contributions by Lankford [1] and Hill [2] laid the theoretical foundations of plasticity and introduced key parameters such as the plastic anisotropy coefficient (r) and the strain hardening exponent (n), both of which have been shown to exert a strong influence on the formability of metallic sheets.

A significant breakthrough in experimental formability characterization emerged in the 1960s with the pioneering work of Keeler and colleagues [3], [4]. By applying a measurement grid on the sheet surface and tracking its deformation up to fracture, they were able to determine the principal strain values corresponding to the onset of failure. Repeating these tests for specimens of various geometries -thus representing different stress and strain states- they introduced the forming limit diagram (FLD), in which the envelope connecting the critical strain points was termed the forming limit curve (FLC). Their investigations initially focused on the positive strain region, ranging from plane strain ($\varepsilon_2 = 0$) to equibiaxial tension ($\varepsilon_2 = \varepsilon_1$). The extension of the diagram to negative minor strains ($\varepsilon_2 < 0$) was later proposed by Goodwin [5], thereby completing the modern representation of the FLD used today.

Over time, Keeler refined his theoretical framework and adapted it to industrial applications, addressing practical challenges encountered in sheet metal forming processes [6], [7]. The classical experimental determination of FLCs has since been standardized through methods such as the Nakajima [8] and Marciniak tests, differing mainly in punch geometry -the Nakajima test employs a hemispherical punch, while the Marciniak test utilizes a flat punch. These tests remain the benchmark for experimental evaluation of forming limits.

Parallel to experimental advancements, several researchers have proposed theoretical and numerical methods to predict the onset of localized necking. Building on the physical understanding of thinning and instability phenomena, Swift, Hill [9], [10] and Stören and Rice [11] formulated

theoretical approaches for estimating forming limit curves under plane stress conditions. More recently, Abspoel et al. [12] developed a statistical model which considers so-called r-value (Lankford-coefficient) and correlating the position and shape of the FLC with material parameters obtained from uniaxial tensile tests. Their approach provided a more physically consistent link between measurable mechanical properties and predicted forming limits. Similar model was developed by Kumar [13]. Besides, if somebody talks about theoretical evaluation of FLCs, the work of Hora [14] Keeler-Brazier [15] and Levy and Tyne [16] also has to be mentioned as relevant developments of roughly the last decade.

Despite these extensive efforts, the reliable prediction of FLCs for ultra-high-strength steels (UHSS) -particularly those with tensile strengths exceeding 1200 MPa- remains a challenge. In such materials, the transition between diffuse and localized necking occurs within a very narrow strain range, complicating both experimental detection and theoretical interpretation. This study therefore aims to assess the applicability of established theoretical models, originally validated for lower-strength steels, to a material with tensile strengths up to 1500 MPa. By combining experimental Nakajima tests with theoretical predictions based on both formulations, this work seeks to clarify the predictive limits and potential refinements required for the accurate modeling of UHSS formability.

Materials and Methods

Applied materials.

The materials investigated in this study were two grades of dual-phase (DP) steel sheets with nominal tensile strengths of 800 MPa (DP800) and 1500 MPa (DP1500), both widely used in the automotive industry for structural and safety-relevant components. Dual-phase steels belong to the class of second-generation advanced high-strength steels (AHSS), characterized by a microstructure consisting of a soft ferritic matrix and hard martensitic islands. This combination ensures an advantageous balance between strength and ductility, making DP steels ideal for lightweight vehicle design, where crash performance must be enhanced without significantly increasing weight.

The microstructural characteristics of both steels were examined to determine the phase distribution and grain morphology. The average grain size of the ferritic and martensitic phases was measured to be $Ød_{ave\_f}$ = 4,55 µm and $Ød_{ave\_m}$ = 2,21 µm for DP800, and $Ød_{ave\_f}$ = 8,58 µm and $Ød_{ave\_m}$ =4,24 µm for DP1500. The phase fraction analysis revealed that the martensite content was approximately 38±3% in DP800 and 82±5% in DP1500, respectively. Representative micrographs of the investigated materials are shown in Fig. 1, illustrating the distinct dual-phase structure and grain morphology of each steel.

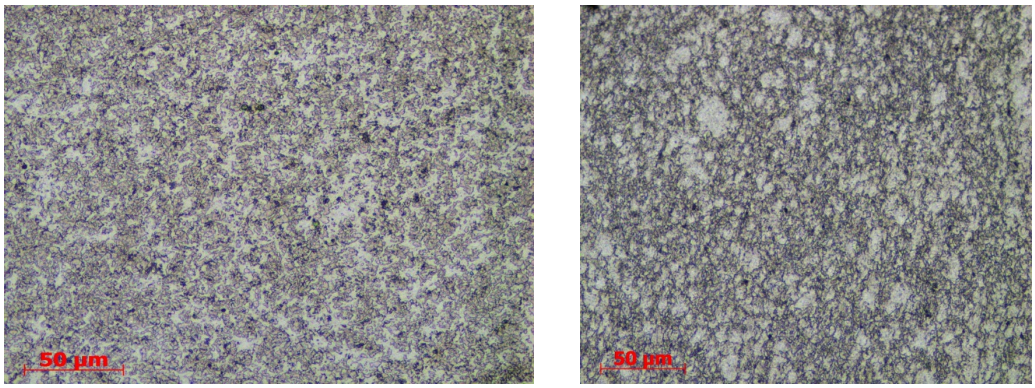

Fig. 1. Microstructure of DP800 (left) and DP1500 (right).

Figure 2 presents the engineering stress-strain curves (σ-ε) and the corresponding true stress-strain curves (σ'-ε') obtained from uniaxial tensile tests at 0° to the rolling direction.

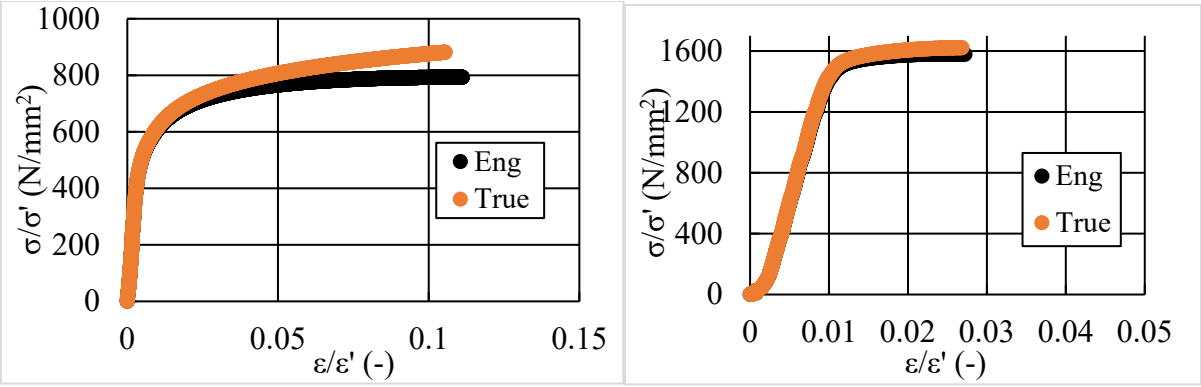

Fig. 2. Stress-strain curves of DP800 (left) and DP1500 (right).

The DP1500 grade exhibits a significantly higher ultimate tensile strength and yield strength, as expected, while the DP800 material maintains superior uniform elongation and strain hardening capability. Figure 3 presents the corresponding flow curves of both materials.

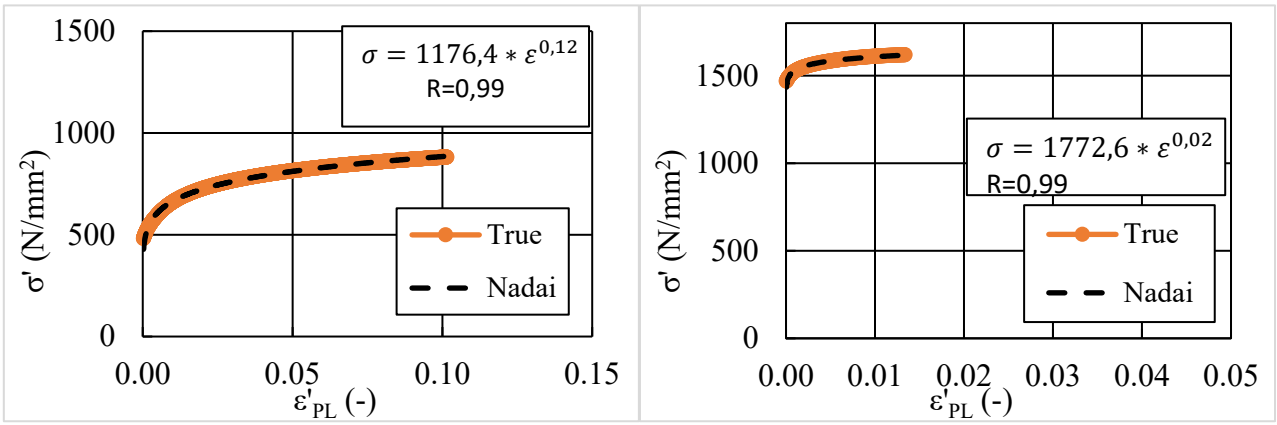

Fig. 3. Flow curves of DP800 and DP1500.

These results reflect the fundamental trade-off between strength and ductility typical for high-strength dual-phase steels. Both materials display a continuous yielding behavior without a distinct yield point, which is characteristic of their mixed ferrite-martensite microstructure. The most important, average mechanical parameters in every 15° to the rolling direction are listed in Table 1.-2.

Table 1. Relevant mechanical parameters of DP800.

DP800						
	A_{80} ave. (-)	A_g ave. (-)	TS ave. (N/mm²)	$R_{p0,2}$ ave. (N/mm²)	r ave. (-)	n ave. (-)
0°	0,152	0,107	857	493	0,817	0,118
15°	0,162	0,115	823	472	0,745	0,123
30°	0,162	0,114	796	451	0,878	0,127
45°	0,166	0,116	770	436	0,876	0,127
60°	0,160	0,116	830	474	0,787	0,125
75°	0,148	0,109	859	452	1,002	0,129
90°	0,148	0,105	831	480	0,862	0,121

Table 2. Relevant mechanical parameters of DP1500.

DP1500						
	A_{80} ave. (-)	A_g ave. (-)	TS ave. (N/mm^2)	$R_{p0,2}$ ave. (N/mm^2)	r ave. (-)	n ave. (-)
0°	0,030	0,019	1556	1438	0,777	0,024
15°	0,035	0,025	1595	1420	0,742	0,038
30°	0,032	0,023	1559	1410	0,503	0,023
45°	0,031	0,023	1521	1370	0,411	0,024
60°	0,026	0,020	1503	1367	0,535	0,023
75°	0,026	0,020	1461	1320	0,822	0,022
90°	0,031	0,021	1441	1287	0,686	0,026

The uniaxial tensile tests were performed on flat specimens cut at orientations of 0°, 15°, 30°, 45°, 60°, 75°, and 90° with respect to the rolling direction. The tests were conducted on an Instron 5900R 4482 universal testing machine equipped with a video extensometer (Instron 5585) to ensure accurate strain measurement. The tests followed the recommendations of ISO 6892-1, with a crosshead speed of 4 mm/min corresponding to an initial strain rate of approximately $8 \cdot 10^{-4}$ s^{-1}.

The resulting data were used to determine key mechanical parameters, including the yield strength ($R_{p0,2}$), ultimate tensile strength (TS), uniform elongation (A_g), and anisotropy coefficients (r-values), which served as input parameters for the theoretical forming limit curve (FLC) calculations. It is worth mentioning that the r-values were continuously measured in the strain range of $A_g \ldots A_g/2$, then those have been averaged. The n-values were calculated according to the Nadai formula [17]:

$$\sigma' = K \cdot \varepsilon'^{n}, \quad (1)$$

in which the K parameter is material dependent strength coefficient.

Forming limit tests (Nakajima tests).

The experimental forming limit curves were determined according to ISO 12004-2 using an ERICHSEN 142-40 universal sheet metal testing machine. The tests were performed at a constant punch movement speed of 20 mm/min, employing a hemispherical punch with a diameter of 100 mm. To obtain a range of strain paths, specimens of different widths were prepared, from narrow to wide, producing conditions from uniaxial to equi-biaxial tension. The initial blank diameter was 220 mm, and the sheet thickness was 1±0,05 mm. The test was terminated when the value of the force dropped by 30%. The geometries of the applied test specimens are listed in Table 3, for which the explanation of the measures is depicted on Fig. 4.

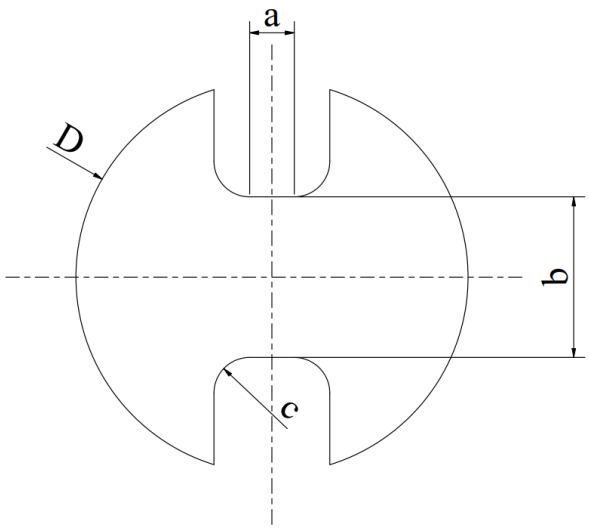

Fig. 4. Parametric view of the applied test specimens.

Table 3. Dimensions of different test specimens.

b (mm)	a (mm)	c (mm)	D (mm)
30	25	20	220
70	25	20	220
80	25	20	220
90	25	20	220
100	25	20	220
110	25	20	220
120	25	20	220
220	-	-	-

To minimize frictional effects and ensure repeatability, a sandwich lubrication method was applied during the Nakajima tests. A polyethylene film (thickness ≈ 0,05 mm) was placed between the die and the specimen, and Luba 251 cold-forming oil was applied on both interfaces with an average coating mass of 79±5 g/m². This lubrication strategy ensured stable frictional conditions and reduced local heating or galling effects during testing.

Data evaluation.

The recorded strain fields (Fig. 5) were post-processed using the Vialux ARGUS software (Fig. 6), following the Volk and Hora methodology [18] to identify the onset of localized necking.

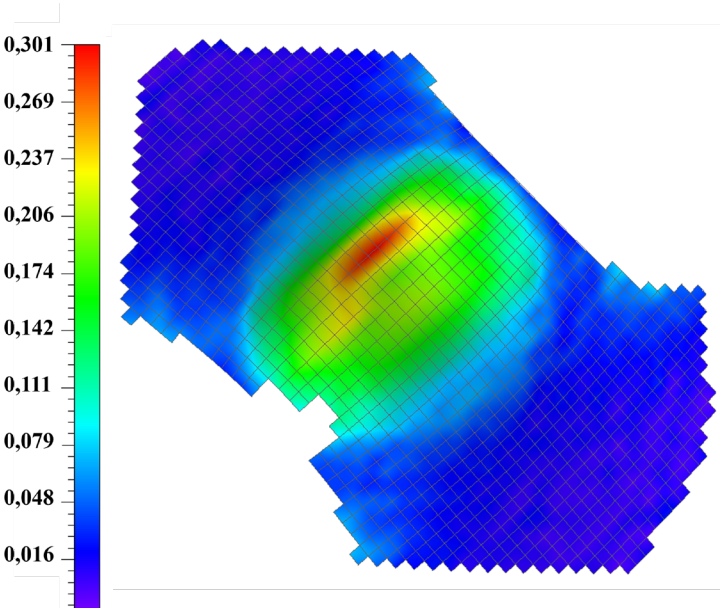

Fig. 5. Strain evaluation of DP800.

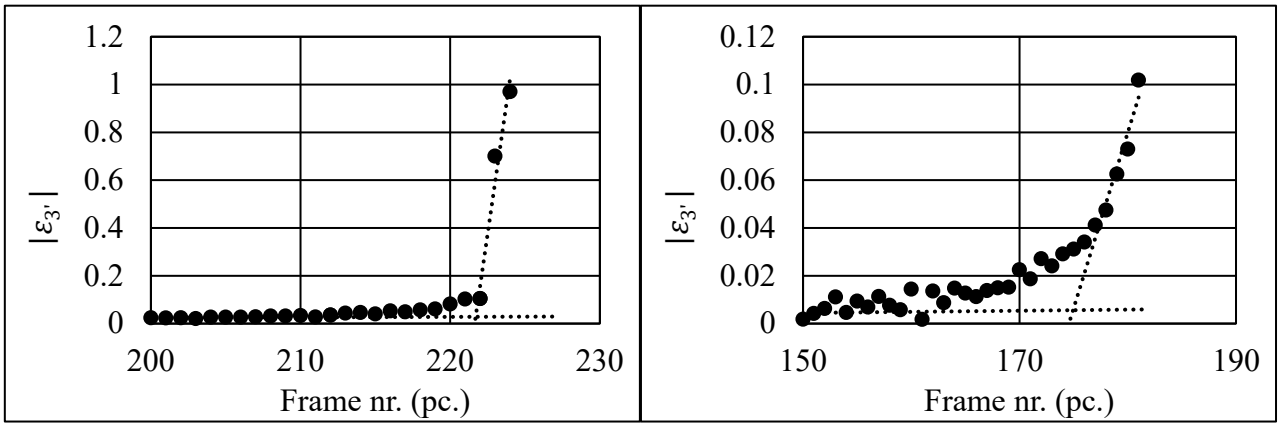

Fig. 6. Identification of the onset of necking for DP800 (left) and DP1500 (right).

For each strain path, the forming limit strain was defined at the point where the the absolute value of the first derivative of the thickness-direction deformation curve exhibited a distinct curvature change corresponding to the initiation of localized necking (Fig. 6). The resulting data were compiled to construct the experimental forming limit diagrams for both materials.

Theoretical framework.

The forming limits of the investigated DP800 and DP1500 steel sheets were determined by combining experimental Nakajima tests and theoretical predictions derived from established forming limit models available in the literature. The experimental forming limit diagrams were evaluated according to the methodology proposed by Volk and Hora, which enables a precise and objective identification of the onset of localized necking from full-field strain data. The resulting experimental points for each strain path were later compared with the theoretical forming limit curves predicted by analytical and numerical models.

The theoretical predictions were obtained using MATLAB software, where the analytical equations of some selected instability models were implemented and solved for the material parameters determined from the uniaxial tensile tests. The graphical representation of the calculated curves allowed for a direct visual comparison between the predicted and experimentally measured forming limits.

The investigated theoretical frameworks include both formulation. The Stören-Rice model doesn't include the r-value in itself. The governing criterion of this model can be expressed as:

$$\varepsilon_1 = \frac{[3\rho^2+n(2+\rho)^2]}{[2(2+\rho)*(1+\rho+\rho^2)]}, \tag{2}$$

$$P = \frac{d\varepsilon_2}{d\varepsilon_1};\ (-1 \le \rho \le 1). \tag{3}$$

Here, the major strain (ε_1) is calculated theoretically, and the belonging minor strain (ε_2) is expressed by the strain ratio: ρ.

In addition to this, formulation proposed by Abspoel et al. [12] -which takes the r-value into consideration- was implemented, which introduces the influence of plastic anisotropy and total elongation through experimentally measurable material parameters, such as the Lankford coefficients (r). The final equations for the critical strains at necking in different stress states are the following.
Uniaxial stress state:

$$\varepsilon_1 = (1 + 0{,}797 * r^{0{,}701}) * \frac{\left(0{,}0626*A_{80}^{0{,}567}+(t-1)*(0{,}12-0{,}0024*A_{80})\right)}{\sqrt{(1+(0{,}797*r^{0{,}701})^2}}, \tag{4}$$

$$E_2 = \frac{(0{,}0626*A_{80}^{0{,}567}+(t-1)*(0{,}12-0{,}0024*A_{80}))}{\sqrt{(1+(0{,}797*r^{0{,}701})^2}}. \tag{5}$$

Plane strain stress state:

$$\varepsilon_1 = 0{,}0084 * A_{80} + 0{,}0017 * A_{80} * (t-1). \tag{6}$$

Equi-biaxial stress state:

$$\varepsilon_1 = \varepsilon_2 = 0{,}00215 * A_{80}^{MIN} + 0{,}25 + 0{,}00285 * A_{80}^{MIN} * t\ . \tag{7}$$

Intermediate-biaxial stress state:

$$\varepsilon_1 = 0{,}0062 * A_{80} + 0{,}18 + 0{,}0027 * A_{80} * (t-1), \tag{8}$$

$$\varepsilon_2 = 0{,}75 * \left(0{,}0062 * A_{80} + 0{,}18 + 0{,}0027 * A_{80} * (t-1)\right). \tag{9}$$

These two approaches represent fundamentally different assumptions regarding the material's plastic response. The Stören-Rice model neglects the directional dependence of plastic flow, while the Abspoel formulation accounts for the evolution of plastic strain anisotropy during deformation. Although, the r-value appears in the functions of the uniaxial stress state only according to the formulations of Abspoel et al., there is a significant difference between the nature of the equations.

Authors know that this is an arbitrary selection of existing theoretical models, but the comparison of these models therefore could provide valuable insight into the significance of anisotropy effects in predicting forming limits, particularly for ultra-high-strength steels (UHSS) where texture and microstructural effects are more pronounced.

Results

The experimental results obtained from the Nakajima tests revealed consistent deformation and fracture behavior for both investigated steels. Figure 7. presents the experimental FLCs of both materials.

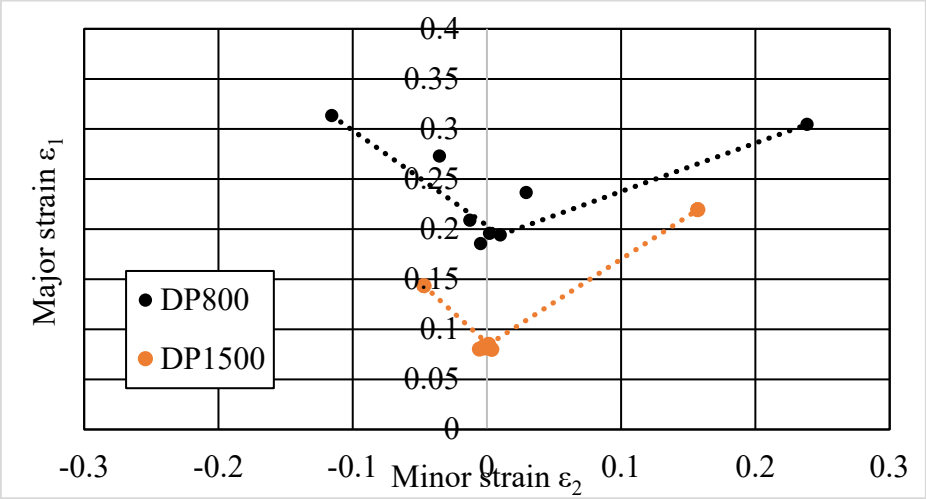

Fig. 7. Experimental FLCs of DP800 and DP1500.

The experimental scatter of the major strain at the onset of localized necking was found to be small, with a maximum deviation of ±5% across repeated measurements.

The phase fraction analysis revealed a martensite content of 38±3% in DP800 and 82±5% in DP1500, indicating that DP1500 contains approximately twice as much martensite as DP800. This significant increase in martensite fraction leads to higher strength but reduced strain hardening capability, as reflected by the fitted hardening exponents (n≈0.12 for DP800 vs. n≈0.02 for DP1500).

Consequently, the forming limit diagram of DP1500 is consistently shifted downward compared to DP800. In the near plane-strain region ($\varepsilon_2 \approx 0$), the major strain (ε_1) of DP800 is approximately twice that of DP1500, which correlates well with the nearly doubled martensite content of DP1500.

The equivalent strain results support this trend: DP800 exhibits equivalent-strain values predominantly in the range of ~0.21-0.32 (average ≈0.29), whereas DP1500 shows substantially lower characteristic values around ~0.09-0.15 (average ≈0.14) in several geometries. This indicates earlier strain localization in DP1500, which can be directly linked to its high martensite fraction and limited work hardening capacity.

Table 4. Avaraged values of major and minor strains.

b (mm)	30		60		70		80	
Strain	ε_1	ε_2	ε_1	ε_2	ε_1	ε_2	ε_1	ε_2
DP800	0,313	-0,116	0,273	-0,035	0,209	-0,013	0,185	-0,005
DP1500	0,143	-0,047	0,080	-0,005	0,081	-0,002	0,083	-0,002
b (mm)	90		100		120		220	
Strain	ε1	ε2	ε1	ε2	ε1	ε2	ε1	ε2
DP800	0,196	0,002	0,194	0,010	0,237	0,029	0,305	0,238
DP1500	0,082	0,000	0,085	0,001	0,080	0,004	0,219	0,157

The comparisons of the theoretical and experimental curves are shown by Fig. 8 and 9. The calculations have been carried out in both 0° and 90° to the rolling direction.

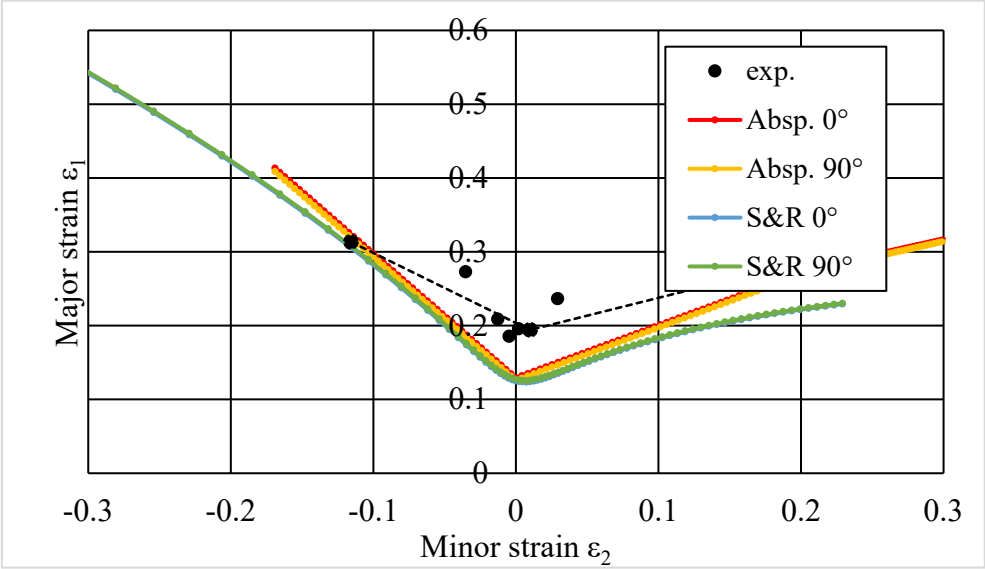

Fig. 8. Experimental and theoretical FLCs of DP800.

The difference between the calculated curves of different tensile test specimen orientation is negligible, because of the similarities in plastic anisotropy. The n and A_{80} values are also very similar in these orientations, for both materials. However, their matching with the experimental results is not very convincing close to the plane strain state. Exactly on the axis of $\varepsilon_2 = 0$, significant deviation can be observed.

Away from the zero minor strain axis, the fit of the experimental and theoretical results is considered good in the positive quadrant of the FLCs. Roughly the same can be stated for the left-hand side of the FLCs, too.

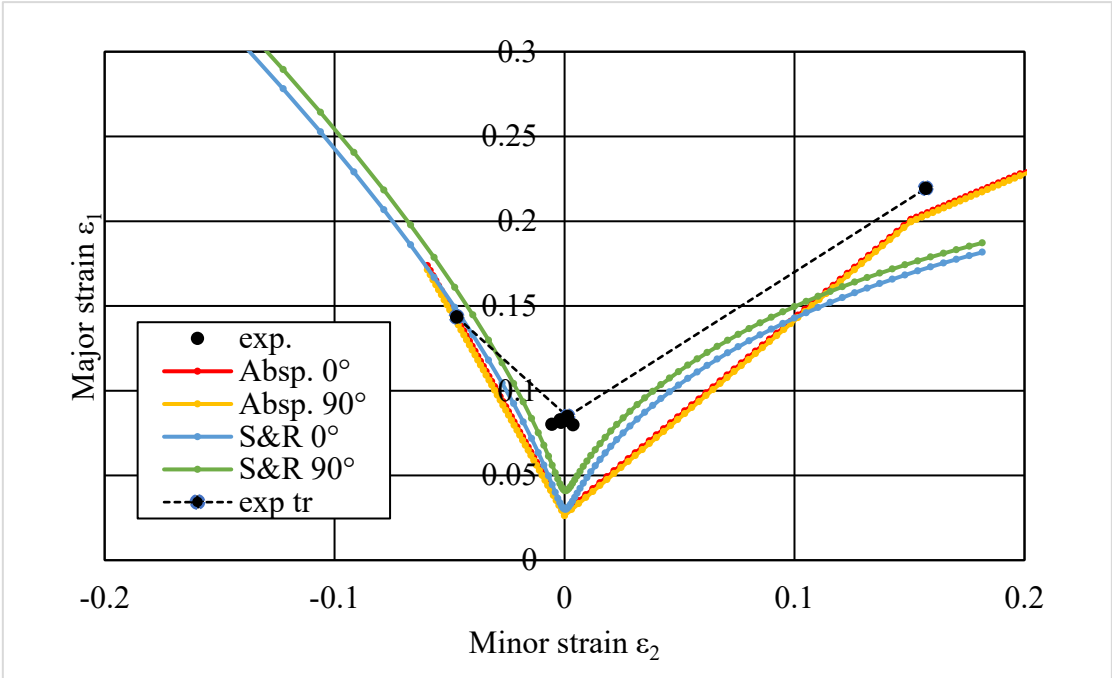

Fig. 9. Experimental and theoretical FLCs of DP1500.

The predictive performance of the investigated models was quantified using the mean absolute percentage error (MAPE), which expresses the average relative deviation between the calculated and experimentally determined forming limit values. The MAPE was calculated according to

$$\mathrm{MAPE} = \frac{1}{\mathrm{N}} * \sum_{\mathrm{i}} \left| \frac{\varepsilon_{1,\mathrm{pred,i}} - \varepsilon_{1,\mathrm{meas,i}}}{\varepsilon_{1,\mathrm{meas,i}}} \right| * 100\% \quad (10)$$

Where $\varepsilon_{1,\mathrm{meas,i}}$ and $\varepsilon_{1,\mathrm{pred,i}}$ denote the measured and predicted major strain values at identical ε_2 positions, respectively, and N is the number of evaluated strain states. The predictive accuracy was then defined as accuracy, = 100 - MAPE.

Based on the global evaluation (including all strain paths), the Abspoel model yielded an accuracy of 78% and 77% for DP800 (0° and 90°), and 75% and 73% for DP1500. The Stören-Rice model resulted in slightly lower values, namely 74% and 74% for DP800, and 73% and 66% for DP1500. These results indicate that the Abspoel approach provides more consistent agreement with the experimental forming limit data, while the predictive capability generally decreases for the higher martensite DP1500 steel.

Since forming limit evaluation is primarily governed by the plane strain region ($\varepsilon_2 \approx 0$), a secondary analysis was performed excluding the extreme biaxial strain states (b = 30 mm and b = 220 mm). Under this restriction, the predictive accuracy decreased for all models. For DP800, the Abspoel model provided 76% and 75% accuracy, while the Stören-Rice model yielded 71% and 71%. For DP1500, the reduction was more pronounced: the Abspoel model achieved 69% and 68%, whereas the Stören-Rice model decreased to 66% and 59% (0° and 90°, respectively). The systematic drop in accuracy in the plane strain region suggests that model performance is more sensitive near the onset of localized instability, particularly for the higher martensite DP1500 steel. This behavior confirms that predictive discrepancies become more significant under strain states most relevant to forming limit determination.

The deviation of the measured and calculated values in plane strain state can be explained by the following assumptions.

1. The less the plastic strains, the more sensitive they are for the difference come from the in-plane and out-of-plane loading.
2. The less the plastic strains, the more sensitive the measurement method is for the dimensions of the measuring grid pattern.
3. None of the n-value and the A_{80} really reflect the material behavior in plane strain state.

To overcome these questions, measurement series are planned for investigating the failure with different grid pattern geometry, applying on Nakajima, uniaxial tension and (in-plane) plane strain tension tests, supported with DIC.

Conclusion

Theoretical and experimental investigations have been executed on forming limit curves of high-strength steels. The comparison between the experimental and theoretical FLCs shows that for the DP1500 steel, both type of models predict the right-hand side (biaxial tension region) of the curve with quite high accuracy. However, near the plane strain condition, a systematic deviation was observed -both models tend to underestimate the experimentally measured forming limits. This deviation indicates that while the theoretical approaches remain valid for high-strength steels under equibiaxial tension, their predictive capability under near-plane strain conditions may require further refinement.

Acknowledgement

We acknowledge the professional support of the Ministry of Culture and Innovation's New National Excellence Program (grant code EKÖP-2024-00020), financed from the National Research, Development and Innovation Fund of Hungary.

References

[1] W. Lankford, S.C. Snyder, J.A. Bauscher, Trans. ASM 42 (1950).

[2] R. Hill, A theory of the yielding and plastic flow of anisotropic metals, Proc. R. Soc. Lond. A 193 (1948) 281-297.

[3] S.P. Keeler, Determination of forming limits in automotive stampings, SAE Trans. 75 (1966).

[4] S.P. Keeler, W.A. Backofen, Plastic instability and fracture in sheet stretched over rigid punches, Trans. ASM 56 (1963) 25-48.

[5] G.M. Goodwin, Application of strain analysis to sheet metal forming problems in the press shop, SAE Paper No. 680092 (1968).

[6] S.P. Keeler, Society of Automotive Engineers, report on metal forming (1968).

[7] S.P. Keeler, Circle grid analysis, National Steel Corp., Livonia, Michigan, 1968.

[8] K. Nakajima, T. Kikuma, Yamata Technical Report 284 (1971).

[9] H.W. Swift, Plastic instability under plane stress, J. Mech. Phys. Solids 1 (1952) 1-18.

[10] R. Hill, On discontinuous plastic states with special reference to localized necking in thin sheets, J. Mech. Phys. Solids 1 (1952) 19-30.

[11] S. Stören, J.R. Rice, Localized necking in thin sheets, J. Mech. Phys. Solids 23 (1975) 421-441.

[12] M. Abspoel, M.E. Scholting, J.M.M. Droog, A new method for predicting forming limit curves from mechanical properties, J. Mater. Process. Technol. 213 (2013) 759-769.

[13] S.K. Paul, Prediction of complete forming limit diagram from tensile properties of various steel sheets by a nonlinear regression based approach, J. Manuf. Process. 23 (2016) 192-200.

[14] P. Hora, L. Tong, B. Berisha, Modified maximum force criterion, a model for the theoretical prediction of forming limit curves, Int. J. Mater. Form. 6 (2013) 267-279.

[15] S. Keeler, M. Kimchi, P.J. Mooney, Advanced high-strength steels, application guidelines, WorldAutoSteel, 2017.

[16] B.S. Levy, C.J. Van Tyne, Determination of a stress-based forming limit curve from mechanical properties, in: IDDRG Conference, Shanghai, China, 2015.

[17] Á. Nádai, A.M. Wahl, E.C. Bingham, Plasticity, a mechanics of the plastic state of matter, J. Rheol. 2 (1931) 455-456.

[18] W. Volk, P. Hora, New algorithm for a robust user-independent evaluation of beginning instability for the experimental FLC determination, Int. J. Mater. Form. 4 (2011) 339-346.